Received: 6 March 2020 | Revised: 13 April 2020 | Accepted: 26 April 2020

DOI: 10.1002/aoc.5806

FULL PAPER

Applied Organometallic Chemistry WILEY

# Antibacterial activity of a new class of tris homoleptic Ru (II)-complexes with alkyl-tetrazoles as diimine-type ligands

**Nicola Monti**[1] | **Stefano Zacchini**[1] | **Massimiliano Massi**[2] | **Alejandro Hochkoeppler**[3,4] | **Loris Giorgini**[1] | **Valentina Fiorini**[1] | **Alessandra Stefan**[3,4] | **Stefano Stagni**[1]

[1]Department of Industrial Chemistry "Toso Montanari", University of Bologna, Viale Risorgimento 4, Bologna, I-40136, Italy

[2]Curtin Institute for Functional Molecules and Interfaces, School of Molecular and Life Science, Curtin University, Kent Street, Bentley, WA, 6102, Australia

[3]Department of Pharmacy and Biotechnology, University of Bologna, Viale Risorgimento 4, Bologna, I-40136, Italy

[4]CSGI, Department of Chemistry, University of Florence, Sesto Fiorentino, FI, I-50019, Italy

**Correspondence**
Valentina Fiorini and Stefano Stagni, Department of Industrial Chemistry "Toso Montanari", University of Bologna, Viale Risorgimento 4, I-40136 Bologna, Italy.
Email: valentina.fiorini5@unibo.it; stefano.stagni@unibo.it

Alessandra Stefan, Department of Pharmacy and Biotechnology, University of Bologna, Viale Risorgimento 4, I-40136 Bologna, Italy.
Email: alessandra.stefan@unibo.it

**Funding information**
Italian Ministry of Education, University and Research (MIUR), Grant/Award Number: PRIN 2015 20154X9ATP_003

Herein, we describe a new family of tris chelate homoleptic Ru (II) complexes, **[Ru(N ℕ)$_3$]$^{2+}$**, where the role of the diimine-type ligands (N ℕ) was fulfilled by 2-pyridyl (PTZ) or 2-quinolyl tetrazole (QTZ) derivatives decorated with various alkyl substituents at the N-2 position of the tetrazole ring. The new Ru (II) complexes with general formula **[Ru (PTZ-R)$_3$]$^{2+}$** and **[Ru (QTZ-R)$_3$]$^{2+}$**, were obtained as mixtures of facial (*fac*) and meridional (*mer*) isomers, as suggested by NMR ($^1$H, $^{13}$C) experiments, and confirmed in the case of ***mer*-[Ru (QTZ-Me)$_3$]$^{2+}$**, by X-ray crystallography. The photophysical behavior of the tetrazole-based **[Ru(N ℕ)$_3$]$^{2+}$** type species was investigated by UV–vis absorption spectroscopy, providing trends typical of polypyridyl Ru (II) complexes. The new homoleptic complexes *fac/mer*-**[Ru (PTZ-R)$_3$]$^{2+}$** and *fac/mer*-**[Ru (QTZ-R)$_3$]$^{2+}$** have been assessed for any eventual antimicrobial activity towards two different bacteria such as Gram-negative *Escherichia coli* and Gram-positive *Deinococcus radiodurans*. Whereas being inactive toward *E. coli*, the response of agar disks diffusion tests suggested that some of the new *fac/mer* Ru (II) complexes could inhibit the growth of *D. radiodurans*. This effect was further investigated by determining the growth kinetics in liquid medium of *D. radiodurans* exposed to the *fac/mer*-**[Ru (PTZ-R)$_3$]$^{2+}$** and *fac/mer*-**[Ru (QTZ-R)$_3$]$^{2+}$** complexes at different concentrations. The outcome of these experiments highlighted that the turn-on of the growth inhibitory effect took place as the linear hexyl chain was appended to the PTZ or QTZ scaffold, suggesting also how the inhibitory activity appeared more pronouncedly exerted by the facial isomers *fac*-**[Ru (PTZ-Hex)$_3$]$^{2+}$** and *fac*-**[Ru (QTZ-Hex)$_3$]$^{2+}$** (MIC = *ca.* 3.0 μg/ml) with respect to the corresponding meridional isomers (MIC = *ca.* 6.0 μg/ml).

**KEYWORDS**

Antibacterials, Deinococcus radiodurans, gram-positive bacteria, ruthenium (II) complexes, Tetrazoles

  

## 1 | INTRODUCTION

The presence of Ru (II) complexes is ubiquitous in studies focused on solar light harvesting, material sciences[1] and bio-imaging.[2] However, tris-homoleptic Ru (II) polypyridyl complexes with the general formula **[Ru(N ℕ)$_3$]$^{2+}$** have been recognized as potential antimicrobial agents for a long time.[3] In particular, even though the bactericidal properties of the of the archetypal complexes [Ru (phen)$_3$]$^{2+}$ and [Ru (bpy)$_3$]$^{2+}$ – where (phen) and (bpy) denote diimine chelators such as 1,10 phenanthroline and 2,2′ bipyridine - were first described in the early 1950's by Dwyer and coworkers,[4a,b] the exploitation of these substitution inert mono and dinuclear Ru (II) polypyridyl complexes as viable alternatives to traditional organic drugs became effective a few decades later, when the ensuing and continued emergence of antibiotic resistant bacteria prompted the search for new classes of antimicrobials. In this regard, chemical modifications of (phen) ligands set and/or the introduction of different ancillary ligands (L Ł), has led to a number of homoleptic **[Ru(N ℕ)$_3$]$^{2+}$** or heteroleptic **[Ru(N ℕ)$_2$(L Ł)]$^{2+}$** – type mononuclear complexes active towards Gram-positive bacteria such as *Staphylococcus aureus* and its methicillin resistant variant MRSA. Furthering these promising results, Keene and coworkers have reported a family of dinuclear Ru (II) complexes – whose structure consists of two peripheral Ru (II) tris-diimine units tethered by alkyl chains with different lengths – as the most effective Ru (II)-based antimicrobial agents, which were active against both Gram-positive (*S. aureus* and MRSA, MIC = 1 μg/ml) and, importantly, Gram-negative bacteria (*i.e. Escherichia coli*, MIC = 1 μg/ml).[5] Therefore, even though the antibacterial activity of metal complexes is likely governed by a delicate balance of sometimes contrasting factors (*i.e.* lipophilicity and global net charge), a consistent research effort has been addressed to extend these studies into other classes of octahedral metal complexes such as Ir (III)-cyclometalates,[6] and to the decoration of the Ru (II) ion with different types of diimine chelators. In these regards, Crowley and coworkers have recently investigated various 1,2,3 triazolyl pyridine containing various alkyl substituents as N ℕ ligands for a family of homoleptic Ru (II) complexes that showed an efficient antimicrobial activity towards Gram-positive bacteria such as MRSA.[7a] Within the general framework of our interests about the application of metal tetrazole complexes in life sciences,[8] we have recently shown that whereas neutrally charged Ir (III) tetrazolato complexes could be employed as luminescent labels for *in vivo* imaging of bacteria,[9] the corresponding series of cationic Ir (III)-tetrazole complexes – enlightening a behavior very similar to that reported by Chao and coworkers for analogous cationic Ir (III) cyclometalates exposed to Gram-positive *Staphylocccus aureus* – [6a] exhibited remarkable antimicrobial activity towards Gram-positive *Deinococcus radiodurans*,[10] a non-pathogenic bacterium that is known as one of the toughest microorganisms, resistant to radiation, oxidative stress and DNA damage.[11] On these premises, and inspired by the work of Crowley and coworkers,[7a] we have endeavored to design and prepare a new set of homoleptic "fully tetrazole" Ru (II) complexes with the general formula **[Ru(N ℕ)$_3$]$^{2+}$**, to be successively screened for their eventual antimicrobial properties. In particular, the scaffold of the bis chelating diimines (N ℕ) is represented by 2-(tetrazol-5-yl) pyridine (**PTZ**) or 2-(tetrazol-5-yl)quinoline (**QTZ**), both kind of ligands being further decorated at the N-2 position of the tetrazole ring with alkyl chains with different length (Scheme 1). Following the approach that we have adopted in our recent works, the antimicrobial features of the resulting families of Ru (II) complexes, namely *fac/mer*-**[Ru (PTZ-R)$_3$]$^{2+}$** and *fac/mer*-**[Ru (QTZ-R)$_3$]$^{2+}$**, have been studied towards Gram-negative *Escherichia coli* and, aiming at exploring the use of a not pathogenic alternative to *Staphylococcus aureus*, with respect to Gram-positive *Deinococcus radiodurans.*

## 2 | RESULTS AND DISCUSSION

The synthetic procedures that were followed for the preparation of the homoleptic Ru (II) complexes are outlined in Scheme 2.

The N-2 alkylated tetrazoles employed in this work were prepared according to a two steps procedure that involved the preliminary formation of the pyridyl and quinolyl tetrazoles,[12] followed by the addition of the desired alkyl moieties.[13a–c] It has to be noted that the latter reaction usually produces a mixture of comparable amounts of two alkylated regioisomers[14] in which the

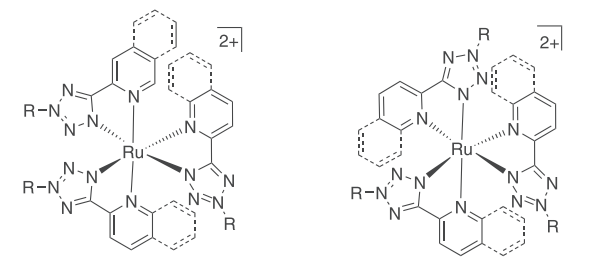


*mer*
R = $CH_3$, *mer*-[Ru(PTZ/QTZ-Me)$_3$]$^{2+}$
R = C-$(CH_3)_3$, *mer*-[Ru(PTZ/QTZ-$^t$Bu)$_3$]$^{2+}$
R = $CH_2$-$(CH_2)_4$-$CH_3$, *mer*-[Ru(QTZ-Hex)$_3$]$^{2+}$

*fac*
R = $CH_3$, *fac*-[Ru(PTZ/QTZ-Me)$_3$]$^{2+}$
R = C-$(CH_3)_3$, *fac*-[Ru(PTZ/QTZ-$^t$Bu)$_3$]$^{2+}$
R = $CH_2$-$(CH_2)_4$-$CH_3$, *fac*-[Ru(QTZ-Hex)$_3$]$^{2+}$

**SCHEME 1** Ru (II) complexes studied in this work with the corresponding abbreviations

**SCHEME 2** Synthetic routes to the alkylated tetrazoles and to the corresponding Ru (II) complexes

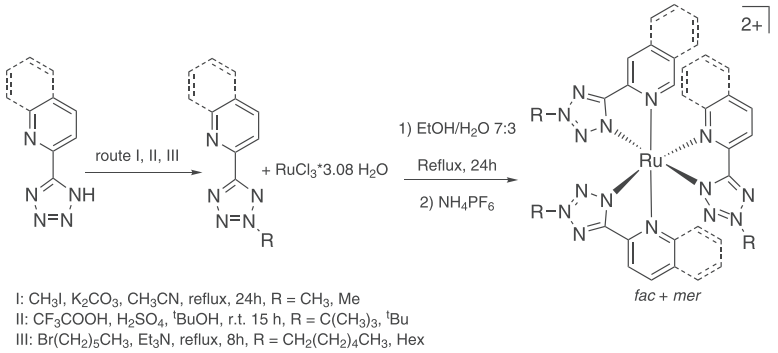


alkyl residue can be bound either to the tetrazole N-1 or N-2 position. Aiming at using the N-2 alkylated tetrazoles as analogues of (bpy) or (phen)– type ligands, their purification from the N-1 isomers was accomplished through column chromatography. Therefore, the corresponding homoleptic Ru (II) complexes were prepared by treating hydrate $RuCl_3$ with a slight molar excess of the appropriate N-2 alkyl tetrazole in a mixture of ethanol and water (7:3 *v*/v) at the reflux temperature. After a counterion exchange procedure aimed at replacing chlorides with two hexafluorophosphate anions, each of the resulting complexes was recovered as a statistical mixture of facial (*fac)* and meridional (*mer)* isomers, whose occurrence was determined from the analysis of the $^1$H NMR spectra (Figure S13-S24 SI†; $^{13}$C: Figure S25-S36 SI†). Whereas in the *fac* isomers the three ligands are magnetically equivalent – displaying therefore a pattern of signals congruent with one single ligand – the lower symmetry of the *mer* isomers generates splitting of the resonance of each individual hydrogen atom into three distinct signals (Figure 1). The isolation of the pure isomers was accomplished by column chromatographies by using silica or alumina as the stationary phase. The separation of the *fac* and *mer* isomers was successful for all of the mixtures with the exception of ***fac*-[Ru (QTZ-Hex)$_3$]$^{2+}$**, which was isolated in combination with the corresponding *mer*-isomer even after repeated attempts (*fac/mer* = 80:20 from $^1$H-NMR data).

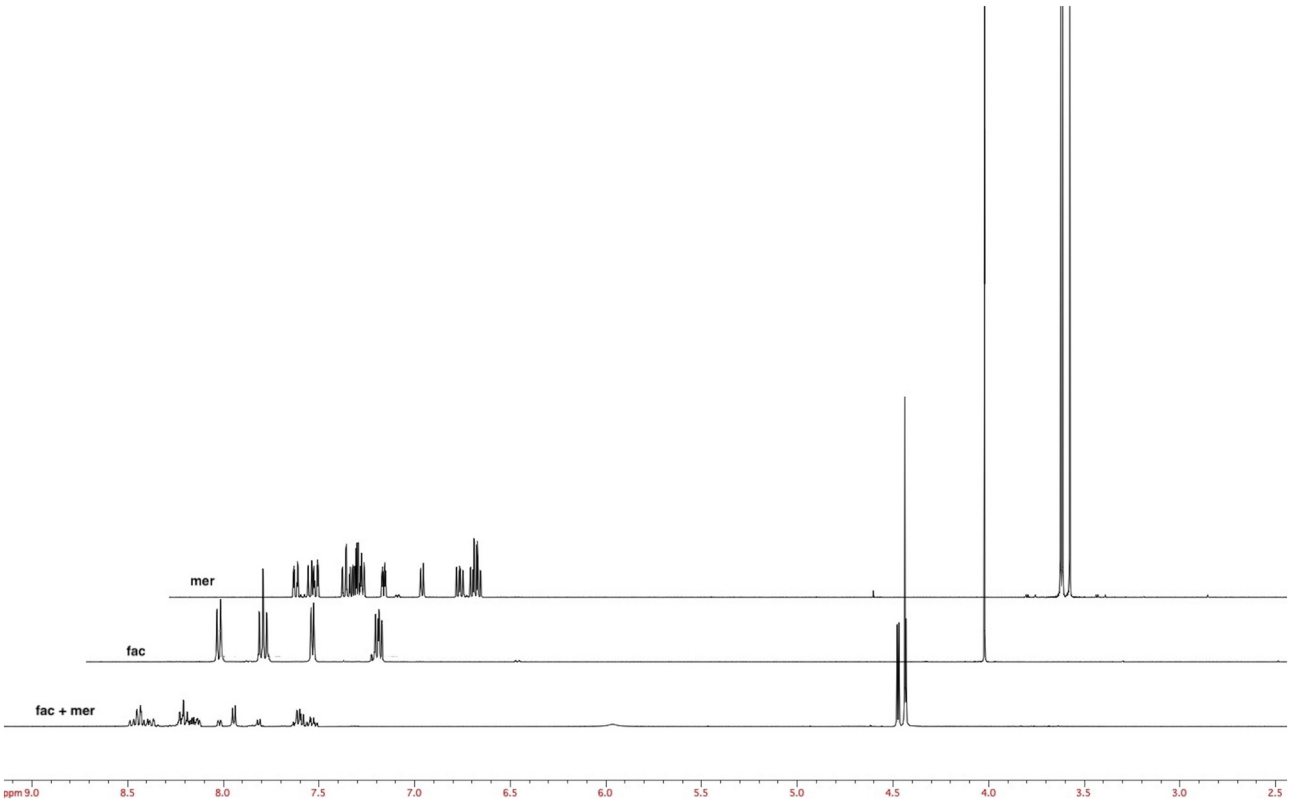


**FIGURE 1** selected NMR spectra of **[Ru (PTZ-Me)$_3$]$^{2+}$** as mixtures of *mer/fac* isomers before and after purification

## 2.2 | X-ray crystallography

Among the series of the Ru (II) complexes, only the one that was suggested as ***mer*-[Ru (QTZ-Me)$_3$]$^{2+}$** afforded single crystals suitable for X-ray diffraction (Figure 2, Table 1, and Supporting Information, SI†, Table S3). The analysis of its molecular structure (Figure 2 and Table 1) provided results congruent with the occurrence of the expected octahedral complex in which the coordination sphere of the Ru (II) ion consisted of three bis chelate (QTZ-Me) ligands arranged in meridional (*mer*) geometry. As expected from tris chelate complexes, the unit cell of the crystal is represented by a racemic mixture of Δ and Λ enantiomers. In comparison to *mer* isomers of the homoleptic Ru (II) complexes reported by Crowley[7a] the molecular structure of ***mer*-[Ru (QTZ-Me)$_3$]$^{2+}$** evidenced a more pronounced distortion from the octahedral geometry. A closer inspection of the Ru-N bond distances revealed that the ones relative to the Ru-N (tetrazole) bonds in trans position to each other display almost identical distances [Ru(1)-N(6) = 2.044(4) Å, Ru(1)-N(11) = 2.043(5) Å], whereas the Ru-N (tetrazole) bond trans to Ru-N (quinolyl) is sensibly shorter [Ru(1)-N(1) = 2.010(4) Å]. Similarly, the two Ru-N (quinolyl) bonds in relative trans position are identical within the experimental error [Ru(1)-N(5) = 2.130(4) Å, Ru(1)-N(10) = 2.135(4) Å], whereas the Ru-N (quinolyl) bond trans to the tetrazole ligand is significantly longer [Ru(1)-N(15) = 2.222(4) Å]. The three chelating (QTZ-Me) ligands are rather different concerning the coplanarity of the tetrazole and quinolyl ligands. Thus, the (QTZ-Me) ligand comprising N(1) to N(5) is almost coplanar [angle between the least-squares planes of the tetrazole and quinolyl rings = 6.3(3)°]. Conversely, the other two ligands comprising N(6) to N(10) [20.6(2)°] and N(11) to N(15) [20.9(3)°] are not coplanar. These deviations are likely to be due to the presence of the very rigid and bulk quinolyl condensed aromatic systems.

## 2.3 | Photophysical and electrochemical properties

The absorption profiles obtained from dilute acetonitrile solutions at room temperature are representative of d$^6$ octahedral metal complexes,[15] with intense π-π* Ligand Centered (LC) transitions occurring in the UV region of the electromagnetic spectrum followed at lower energy

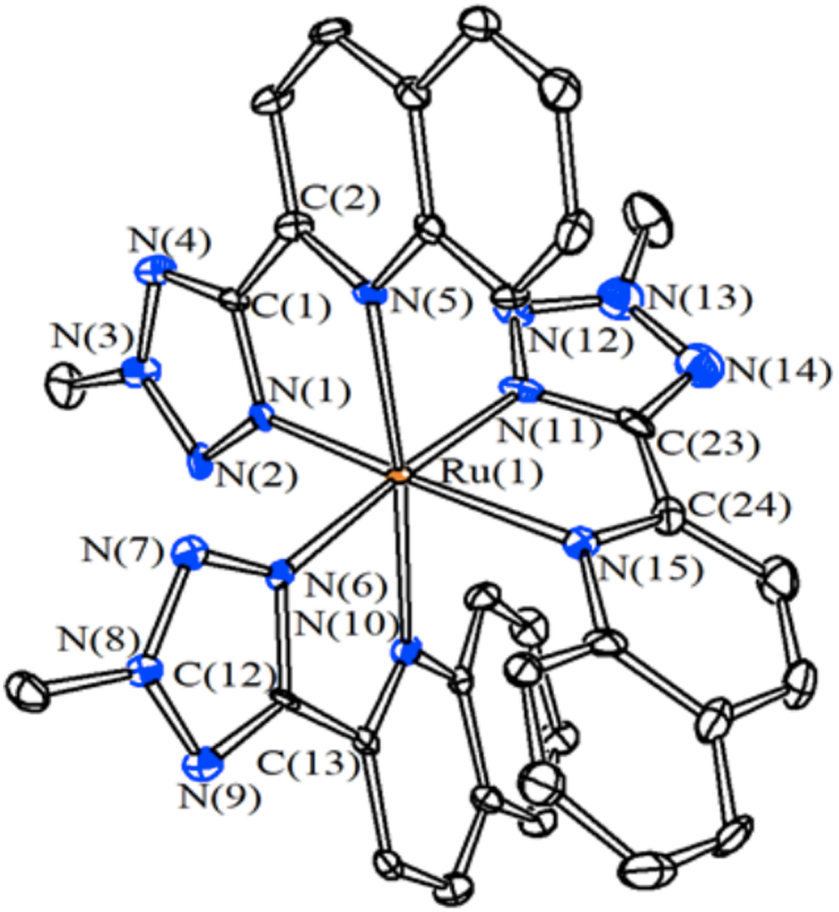


**FIGURE 2** Molecular structure of the dication ***mer*-[Ru (QTZ-Me)$_3$]$^{2+}$** with key atoms labelled. Displacement ellipsoids are at the 50% probability level. H-atoms are omitted for clarity

**TABLE 1** Selected bond lengths (Å) and angles (°) for ***mer*-[Ru (QTZ-Me)$_3$]$^{2+}$**

| | | | | | |
|---|---|---|---|---|---|
| **Ru(1)-N(1)** | **2.010(4)** | **Ru(1)-N(6)** | **2.044(4)** | **Ru(1)-N(11)** | **2.043(5)** |
| Ru(1)-N(5) | 2.130(4) | Ru(1)-N(10) | 2.135(4) | Ru(1)-N(15) | 2.222(4) |
| C(1)-N(1) | 1.345(6) | C(12)-N(6) | 1.352(6) | C(23)-N(11) | 1.331(7) |
| C(1)-N(4) | 1.327(7) | C(12)-N(9) | 1.322(7) | C(23)-N(14) | 1.339(7) |
| N(1)-N(2) | 1.319(6) | N(6)-N(7) | 1.318(6) | N(11)-N(12) | 1.321(6) |
| N(2)-N(3) | 1.325(6) | N(7)-N(8) | 1.337(6) | N(12)-N(13) | 1.328(7) |
| N(3)-N(4) | 1.326(6) | N(8)-N(9) | 1.329(6) | N(13)-N(14) | 1.334(7) |
| C(1)-C(2) | 1.456(7) | C(12)-C(13) | 1.449(7) | C(23)-C(24) | 1.446(8) |
| N(1)-Ru(1)-N(5) | 78.00(17) | N(6)-Ru(1)-N(10) | 77.14(17) | N(11)-Ru(1)-N(15) | 76.67(18) |
| C(1)-N(1)-N(2) | 108.4(4) | C(12)-N(6)-N(7) | 107.5(4) | C(23)-N(11)-N(12) | 108.8(5) |
| N(1)-N(2)-N(3) | 103.4(4) | N(6)-N(7)-N(8) | 104.9(4) | N(11)-N(12)-N(13) | 103.9(5) |
| N(2)-N(3)-N(4) | 115.5(4) | N(7)-N(8)-N(9) | 113.7(4) | N(12)-N(13)-N(14) | 114.7(5) |
| N(3)-N(4)-C(1) | 101.3(4) | N(8)-N(9)-C(12) | 102.5(4) | N(13)-N(14)-C(23) | 101.4(5) |
| N(4)-C(1)-N(1) | 111.3(5) | N(9)-C(12)-N(6) | 111.4(5) | N(14)-C(23)-N(11) | 111.2(5) |
| Rms deviation of $N_4C^a$ least-squares plane | 0.0039 | Rms deviation of $N_4C^b$ least-squares plane | 0.0059 | Rms deviation of $N_4C^c$ least-squares plane | 0.0054 |
| Rms deviation of $Q^a$ least-squares plane | 0.0298 | Rms deviation of $Q^b$ least-squares plane | 0.0626 | Rms deviation of $Q^c$ least-squares plane | 0.0692 |
| Angle between least-squares planes of $N_4C^a$ and $Q^a$ | 6.3(3) | Angle between least-squares planes of $N_4C^b$ and $Q^b$ | 20.6(2) | Angle between least-squares planes of $N_4C^c$ and $Q^c$ | 20.9(3) |

$N_4C^a$ = C(1)N(1)N(2)N(3)N(4) tetrazole ring; $N_4C^b$ = C(12)N(6)N(7)N(8)N(9) tetrazole ring; $N_4C^c$ = C(23)N(11)N(12)N(13)N(14) tetrazole ring; $Q^a$ quinolyl ring containing N(5); $Q^b$ quinolyl ring containing N(10); $Q^c$ quinolyl ring containing N(15).

by the metal-to-ligand charge transfer (MLCT) bands (Figure 3, and Supporting Information, SI†, Table S1, Figure S37 – S42).

If compared to [Ru (bpy)$_3$]$^{2+}$ as the reference compound for tris-chelate [Ru(N ℕ)$_3$]$^{2+}$ – type species, all the Ru (II) tetrazole complexes described herein display blue shifted absorption profiles, enlightening a trend that is most likely explained in consideration of the reduced conjugation of the 5-aryl tetrazole ligands with respect to that of bpy. However, in close similitude with the isostructural Ru (II)-pyridyltriazole-based complexes reported by Crowley,[7a] the **PTZ**-based Ru (II) complexes described herein display the MLCT maxima centred in between 380 and 390 nm (Figure 3 and Table S1 SI†). On passing to the 2-quinolyl analogues, **QTZ**-based complexes, the position of the MLCT band is markedly shifted to lower energy ($\lambda_{max}$ *ca.* 420 nm), an effect that is congruent with the more extended π-conjugation across the aromatic ligand. Relative to both series of complexes, only subtle differences were observed for the *fac* and *mer* pure isomers. Unlike [Ru (bpy)$_3$]$^{2+}$ and [Ru (phen)$_3$]$^{2+}$, all the Ru (II) complexes described herein were not luminescent at room temperature. The lack of emission is most likely to be ascribed to the occurrence of thermally accessible metal-centred (MC) states, therefore preventing the efficient population of potentially emissive MLCT-type states.[11] The electrochemical properties of the Ru (II) complexes were investigated by cyclic voltammetry (CV) in acetonitrile solution at room temperature (see Supporting information, SI†, Table S2). In the region of positive potentials, each of the *fac/mer*-**[Ru (PTZ-R)$_3$]$^{2+}$** and *fac/mer*-**[Ru (QTZ-R)$_3$]$^{2+}$**-type complexes displayed one single and reversible Ru (II)/Ru (III)-based process, with no difference observed between each *fac* and *mer* isomer. Along the series of the PTZ-based complexes, *fac/mer*-**[Ru (PTZ-R)$_3$]$^{2+}$**, this process was found between *ca.* 1.63 V – as in the cases of *fac/mer*-**[Ru (PTZ-$^t$Bu)$_3$]$^{2+}$** – and 1.70 V, as for *fac/mer*-**[Ru (PTZ-Hex)$_3$]$^{2+}$**. The quinolyl analogues *fac/mer*-**[Ru (QTZ-R)$_3$]$^{2+}$** displayed the same metal-based process shifted to more positive potentials, being the corresponding potentials observed to span between ca. 1.72 V (for *fac/mer*-**[Ru (QTZ-$^t$Bu)$_3$]$^{2+}$**) and ca. 1.80 V, as in the cases of *fac/mer*-**[Ru (QTZ-Me)$_3$]$^{2+}$**. An analogous trend was observed in the region of the negative potentials, (see Supporting information, SI†, Table S2), in which the three ligand centred reductions that appeared in each voltammetric wave of the *fac/mer*-**[Ru (PTZ-R)$_3$]$^{2+}$** complexes were found to occur at more positive potentials than those displayed by the *fac/mer*-**[Ru (QTZ-R)$_3$]$^{2+}$** analogues. The analysis of these results suggested that the distinctive features that were observed

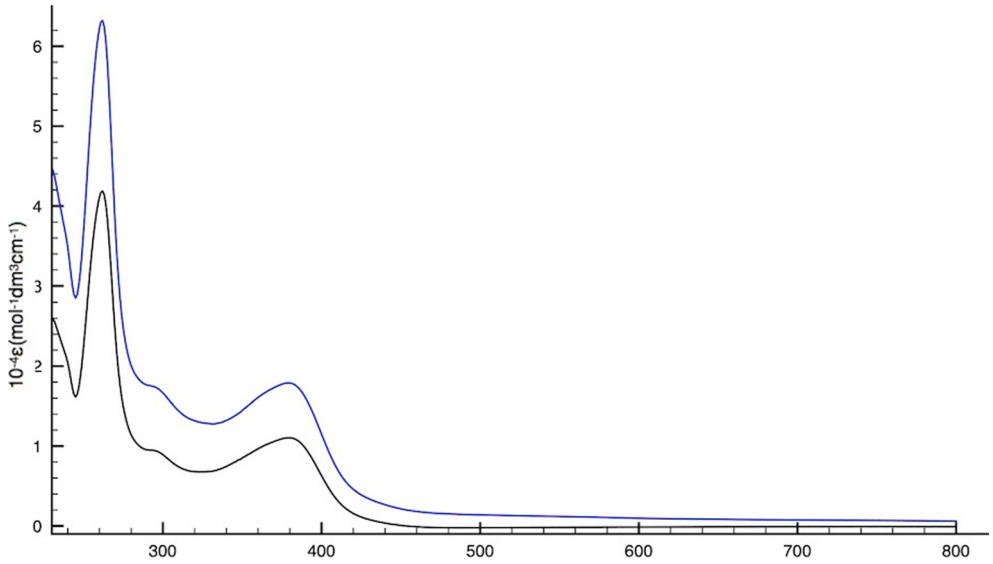


**FIGURE 3** Absorption profiles of ***fac*-[Ru (PTZ-Me)$_3$]$^{2+}$** (blue line) and ***mer*-[Ru (PTZ-Me)$_3$]$^{2+}$** (black line), $CH_3CN$, $10^{-5}$ M, r.t

from the comparison of *fac/mer*-**[Ru (PTZ-R)$_3$]$^{2+}$** and *fac/mer*-**[Ru (QTZ-R)$_3$]$^{2+}$**, were most likely due to the presence of the PTZ or the QTZ-type scaffolds, while no obvious correlations could be made in consideration of the occurrence of alkyl chains with different length and structure.

## 2.4 | Antimicrobial activity

The antimicrobial activity of the *fac/mer*-**[Ru (QTZ-R)$_3$]$^{2+}$** and *fac/mer*-**[Ru (PTZ-R)$_3$]$^{2+}$**-type complexes was investigated against Gram-negative (*Escherichia coli*) and Gram-positive bacteria (*Deinococcus radiodurans*) by performing disk diffusion tests in agar plates followed, in case of positive response, by the broth dilution method to detect potential inhibition of bacterial growth. Given the uncomplete solubility in water displayed by the dicationic Ru (II)-complexes, the corresponding aqueous solutions containing DMSO up to 2% (*v*/v) were used for each testing. In all cases, the results of appropriate control experiments suggested the absence of any DMSO-related observable biological effect. The antimicrobial activity exerted by the Ru (II) complexes was preliminarily assessed by disk diffusion tests in agar plates, in which the appearance of zones of growth inhibition around the paper disks impregnated with *fac/mer*-[Ru(N^N)$_3$]$^{2+}$ complexes was monitored and compared to the output of two further paper disks impregnated with ampicillin and DMSO as positive and negative control, respectively. The growth of *E. coli* was not affected by any of the compounds tested since no visible inhibition haloes appeared, as reported in Figure 4 for *fac/mer*-**[Ru (PTZ-Hex)$_3$]$^{2+}$**.

A completely different response was obtained when the same screening was performed with Gram-positive *D. radiodurans*. In particular, a clear growth inhibition zone did surround the paper disks imbued with *fac/mer*-**[Ru (PTZ-Hex)$_3$]$^{2+}$**, *fac/mer*-**[Ru (QTZ-Hex)$_3$]$^{2+}$** and *mer*-**[Ru (QTZ-$^t$Bu)$_3$]$^{2+}$** (Figure 5), while disks imbued with *fac*-**[Ru (QTZ-$^t$Bu)$_3$]$^{2+}$**, *fac/mer*-**[Ru (PTZ-$^t$Bu)$_3$]$^{2+}$**, *fac/mer*-**[Ru (PTZ-Me)$_3$]$^{2+}$**, and *fac/mer*-**[Ru (QTZ-Me)$_3$]$^{2+}$** did not inhibit bacterial growth.

In a successive stage, the antimicrobial properties of the Ru (II) complexes that displayed a positive outcome in the disk diffusion tests against *D. radiodurans* were further investigated through the analysis of the growth kinetics in liquid medium. For the sake of comparison, also *fac*- and *mer*-**[Ru (QTZ-Me)$_3$]$^{2+}$**, which were suggested to be inactive toward *D. radiodurans* on the basis of agar disks diffusion tests, were included in the series of Ru (II) complexes to be further screened. In the initial set of experiments, independent cultures containing the Ru (II) complexes at concentrations of 5 to 20 μM were prepared and their kinetics of growth were measured and compared to the control cultures.

When *D. radiodurans* cultures were exposed to 20 μM solutions of *fac*- and *mer*-**[Ru (QTZ-Me)$_3$]$^{2+}$** (Figure 6a), a slight decrease of the rate of bacterial growth was observed. In excellent agreement with the outcome of the previous disk diffusion tests, these results suggest that no significant antibacterial activity could be traced back to neither the facial nor the meridional isomer of **[Ru (QTZ-Me)$_3$]$^{2+}$**. On the other hand, the replacement of the methyl group with a tert-butyl moiety, produced a different result. Both *fac*- and *mer*-**[Ru (QTZ-$^t$Bu)$_3$]$^{2+}$** complexes were initially tested by treating individual *D. radiodurans* cultures with 20 μM of each isomer (Figure 6b). A complete inhibition of the bacterial growth was observed in the presence of the *mer*-

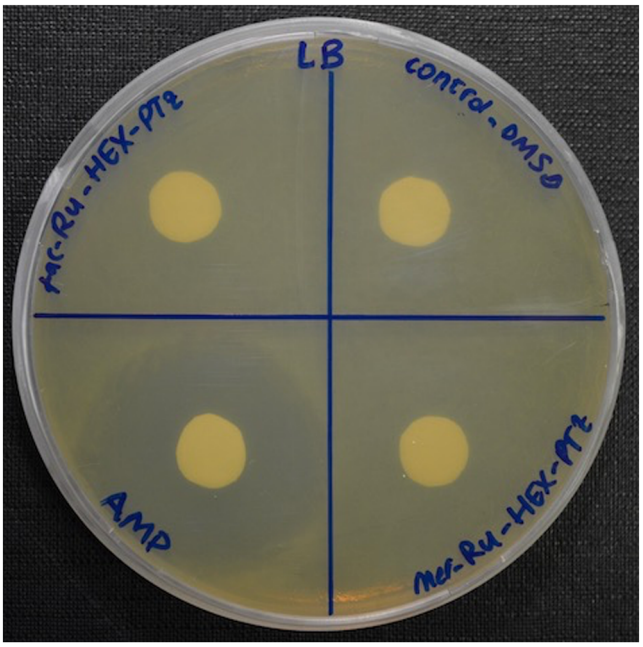


**FIGURE 4** Disk diffusion test for *fac/mer*-**[Ru (PTZ-Hex)$_3$]$^{2+}$** against *E. coli*

**[Ru (QTZ-$^t$Bu)$_3$]$^{2+}$** isomer, while the same concentration of *fac*-**[Ru (QTZ-$^t$Bu)$_3$]$^{2+}$** allowed a poor growth even though prolonged the lag phase (*i.e.* latent period). Conversely, at the lowest concentration limit (5 μM), both *fac* and *mer* **[Ru (QTZ-$^t$Bu)$_3$]$^{2+}$** reduced the rate of bacterial growth at a low extent, with a slightly more pronounced effect exerted by the *mer* isomer. The influence played by the nature of the alkyl residue -**R** in determining the activity of the series of *fac/mer*-**[Ru (QTZ-R)$_3$]$^{2+}$** and *fac/mer*-**[Ru (PTZ-R)$_3$]$^{2+}$**-type complexes toward *D. radiodurans* became evident when the tetrazole rings were decorated with a linear hexyl chain (-**Hex**) to form the ligands abbreviated as **QTZ-Hex** and **PTZ-Hex**, respectively. In particular, *fac/mer*-**[Ru (QTZ-Hex)$_3$]$^{2+}$**, under the form of the pure *mer* isomer and as a mixture of *fac/mer* isomers - as mentioned earlier, samples of pure *fac*-**[Ru (QTZ-Hex)$_3$]$^{2+}$** could not be obtained even after several purification procedures - completely inhibited the growth of *D. radiodurans* both as 20 and 5 μM solutions (Figure 7a), suggesting the occurrence of a strong growth inhibiting action even at their lower concentration limit.[16] Successive experiments were performed in order to evaluate the lowest concentration values at which these latter complexes could exert a significant antibacterial activity. To this extent, *D. radiodurans* cultures were exposed to pure *mer*-**[Ru (QTZ-Hex)$_3$]$^{2+}$** and to the mixture of isomers *fac/mer*-**[Ru (QTZ-Hex)$_3$]$^{2+}$** at the concentration values of 2.5 and 1.0 μM. Whereas pure *mer*-**[Ru (QTZ-Hex)$_3$]$^{2+}$** displayed the same poor antibacterial activity at both of the concentration tested (Figure 7b, green and red lines), the mixture of isomers *fac/mer*-**[Ru (QTZ-Hex)$_3$]$^{2+}$** (Figure 7b, orange and blue lines) induced the complete inhibition of the growth of *D. radiodurans* at the lowest concentration limit of 2.5 μM, highlighting a minimal inhibitory concentration (MIC) of 3.0 μg/ml.

Further in support of the importance of the presence of the hexyl substituent, it was observed that the 2-pyridyl tetrazole-based complexes *fac/mer*-**[Ru (PTZ-Hex)$_3$]$^{2+}$** displayed an antimicrobial activity almost coincident to that determined for their quinolyl tetrazole analogues *fac/mer*-**[Ru (QTZ-Hex)$_3$]$^{2+}$**. Indeed, pure *fac*-**[Ru (PTZ-Hex)$_3$]$^{2+}$** (green and red lines, Figure 8a) and *mer*-**[Ru (PTZ-Hex)$_3$]$^{2+}$** (orange and blue lines, Figure 8a) at the concentration of 20 and 5 μM, completely inhibited the growth of *D. radiodurans*. Also, when *fac* and *mer*-**[Ru (PTZ-Hex)$_3$]$^{2+}$** isomers were

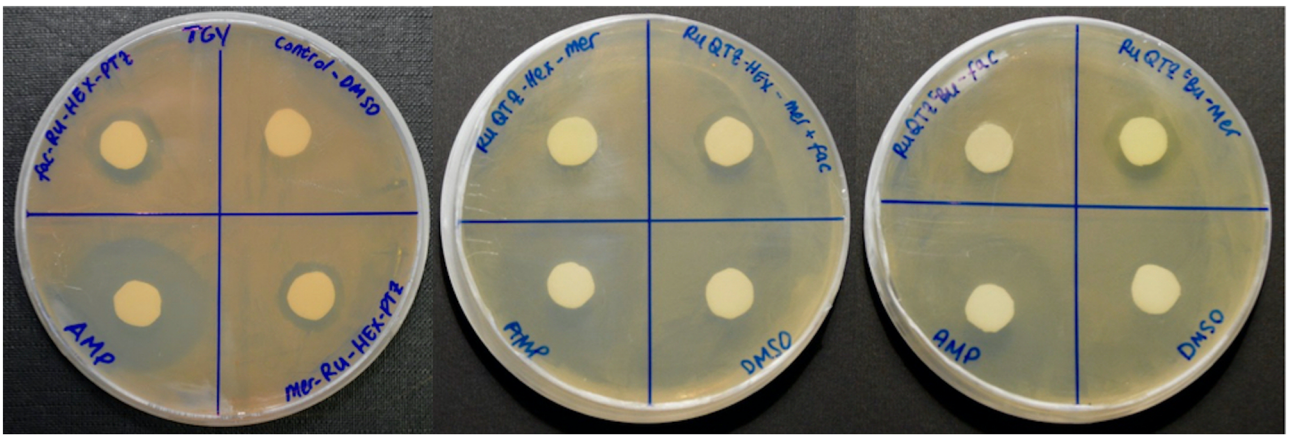


**FIGURE 5** Disk diffusion test for *fac/mer*-**[Ru (PTZ-Hex)$_3$]$^{2+}$**, *fac/mer*-**[Ru (QTZ-Hex)$_3$]$^{2+}$** and *fac/mer*-**[Ru (QTZ-$^t$Bu)$_3$]$^{2+}$** against *D. radiodurans*

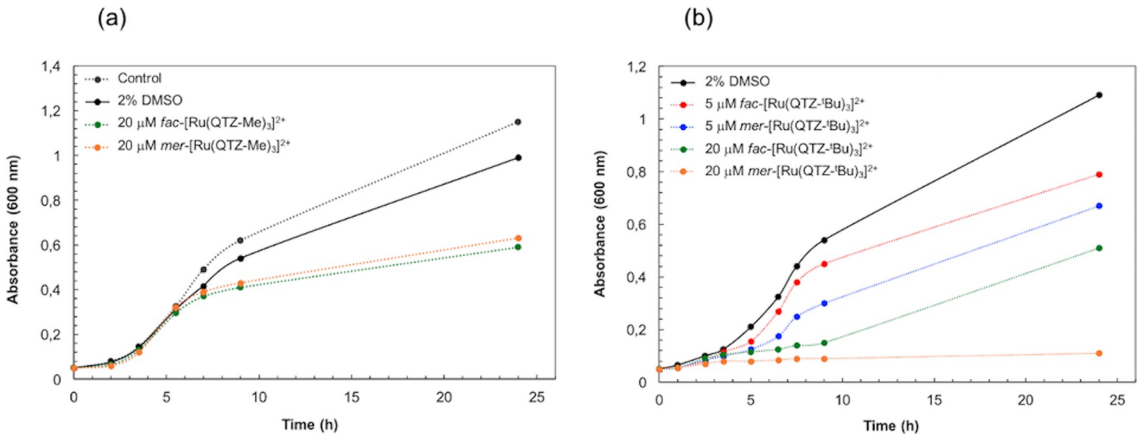


**FIGURE 6** Kinetics of growth of *D. radiodurans* cultures incubated with *fac/mer*-**[Ru (QTZ-Me)$_3$]$^{2+}$** 20 μM (a) and *fac/mer*-**[Ru (QTZ-$^t$Bu)$_3$]$^{2+}$** 5 and 20 μM (b). Control cultures without any complex (black dots) and with 2% DMSO (black curve) were performed

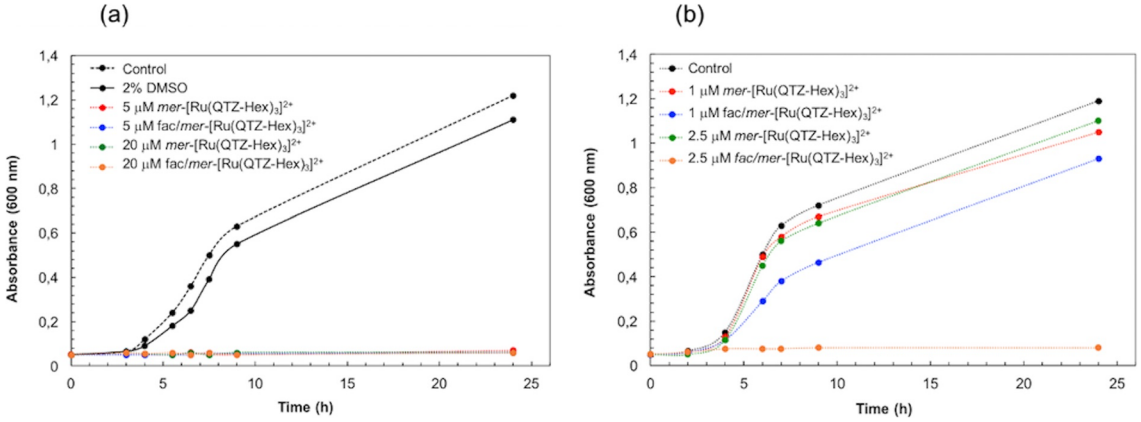


**FIGURE 7** Kinetics of growth of *D. radiodurans* in the presence of *fac/mer*-**[Ru (QTZ-Hex)$_3$]$^{2+}$** at decreasing concentrations: 20 and 5 μM (a), 2.5 and 1 μM (b). Control cultures without any complex (black dots) were performed

tested at lower concentrations (1 and 2.5 μM, Figure 8b), a significant inhibitory effect was detected only in the culture treated with the 2.5 μM solution of the pure isomer *fac*-**[Ru (PTZ-Hex)$_3$]$^{2+}$** (MIC = 3.0 μg/ml), while the growth rate of the remaining cultures – *i.e.* the ones containing 1 μM and 2.5 μM *mer*-**[Ru (PTZ-Hex)$_3$]$^{2+}$** and *fac*-**[Ru (PTZ-Hex)$_3$]$^{2+}$** at the concentration of 1 μM – was not affected (Figure 8b).

Taken together, these results suggest that whereas the choice of PTZ or QTZ-based scaffold is likely not involved in inhibiting the growth of *D. radiodurans,* the proper turn-on of the growth inhibitory effect exerted by the corresponding Ru (II) complexes *fac/mer*-**[Ru (PTZ-R)$_3$]$^{2+}$** and *fac/mer*-**[Ru (QTZ-R)$_3$]$^{2+}$**, takes place when the tetrazole ligands were decorated with a linear hexyl chain (-**Hex**). In addition, the investigation of the antimicrobial properties of *fac/mer*-**[Ru (PTZ-Hex)$_3$]$^{2+}$** and *fac/mer*-**[Ru (QTZ-Hex)$_3$]$^{2+}$** at concentrations below 5 μM suggested how the facial (*fac*) isomers apparently induced the inhibition of the growth of *D. radiodurans* (MIC ca. 3.0 μg/ml) to an extent higher than the one determined for corresponding meridional (*mer*) isomers (MIC ca. 6.0 μg/ml). It is worth noting how our findings about the antimicrobial activity of Ru (II)-tetrazoles derivatives *fac/mer*-**[Ru (PTZ-R)$_3$]$^{2+}$** and *fac/mer*-**[Ru (QTZ-R)$_3$]$^{2+}$** towards *D. radiodurans* share some important features with some previous reports that dealt with the effects deriving from the exposition of mononuclear Ru (II) polypyridyl complexes to different families of Gram-positive bacteria such as *B. subtilis* and, in particular, the pathogenic *S. aureus* and its methicillin resistant variant MRSA.[3,7a] First, the Ru (II)-tetrazole complexes described herein display the same selectivity to Gram-positive *versus* Gram-negative bacteria, the occurrence of which is probably related to the higher permeability of the cell wall of Gram-positive bacteria with respect to the Gram-negative ones. These latter microorganisms are indeed characterized by the presence of an outer membrane mainly composed of lipopolysaccharides (LPS), which likely protects the Gram-negative bacteria

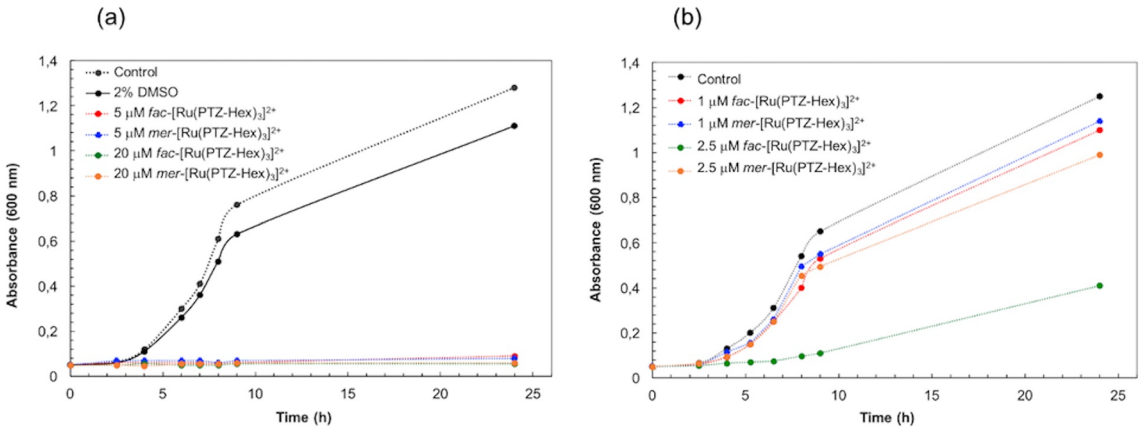


**FIGURE 8** Kinetics of growth of *D. radiodurans* in the presence of *fac/mer*-**[Ru (PTZ-Hex)$_3$]$^{2+}$** at decreasing concentrations: 20 and 5 μM (a), 2.5 and 1 μM (b). Control cultures without any complex (black dots) were performed

from the Ru (II) bis cationic complexes.[3] Furthermore, in a manner identical as that reported by Crowley for Ru (II)pyridyl triazoles exposed to MRSA,[7a] the inhibitory activity towards *D. radiodurans* of our Ru (II) complexes *fac/mer*-**[Ru (PTZ-R)$_3$]$^{2+}$** and *fac/mer*-**[Ru (QTZ-R)$_3$]$^{2+}$** took place upon the introduction of a linear hexyl chain (R = Hex) in the backbone of the tetrazole based ligands. According to the explanations suggested by Crowley,[7a] this specific modification is most likely responsible for endowing the Ru (II) species of the appropriate level of lipophilicity for allowing these Ru (II) complexes to target the bacterial cytoplasmic membrane.

## 3 | CONCLUSIONS

The introduction of one alkyl substituent at the N-2 position of the pentatomic ring of 2-pyridyl (PTZ) and 2-quinolyl tetrazole (QTZ) scaffolds led to a series of diimine-type chelators (N^N) that could be employed for the preparation of the new family of tris-homoleptic "fully tetrazole" [Ru(N^N)$_3$]$^{2+}$ complexes. The formation of the new Ru (II) species with formula **[Ru (PTZ-R)$_3$]$^{2+}$** and **[Ru (QTZ-R)$_3$]$^{2+}$**, respectively, was confirmed by ESI mass spectrometry, and the NMR ($^1$H, $^{13}$C) studies suggested the occurrence of each of the Ru (II) complexes as a statistical mixture of facial (*fac*) and meridional (*mer*) isomers. With the only exception of *fac*-**[Ru (QTZ-Hex)$_3$]$^{2+}$**), the *fac* and *mer* diastereomers were successfully separated by column chromatography, being the structure of one pure isomer, *mer*-**[Ru (QTZ-Me)$_3$]$^{2+}$**, confirmed by single crystal X-ray diffraction. The investigation of the photophysical and electrochemical properties of the new Ru (II) complexes highlighted a behavior that can be traced back to the family of tris-homoleptic Ru (II) polypyridyl complexes, and no significant difference between facial and meridional isomers of each complex was detected. The new families of bis cationic Ru (II) complexes, *fac/mer*-**[Ru (PTZ-R)$_3$]$^{2+}$** and *fac/mer*-**[Ru (QTZ-R)$_3$]$^{2+}$**, were therefore screened for any eventual antimicrobial activity *in vitro* against Gram-negative (*E. coli*) and Gram-positive (*D. radiodurans*) microorganisms. While all Ru (II) complexes were demonstrated as inactive toward *E. coli*, their growth inhibitory effect against *D. radiodurans* – a not pathogenic bacterium that is listed as one of the toughest microorganisms in light of its outstanding resistance to radiation, oxidative stress and DNA damage – appeared to be likely governed by specific structural features. In particular, it was observed the complete inhibition of the growth of *D. radiodurans* upon the introduction of a linear hexyl chain (-**Hex**) in the five membered ring of the PTZ and QTZ ligands, also highlighting how the activity of the facial isomers, *fac*-**[Ru (PTZ-Hex)$_3$]$^{2+}$** and *fac*-**[Ru (QTZ-Hex)$_3$]$^{2+}$** (MIC = *ca.* 3.0 μg/ml) appeared more pronounced than the one displayed by the corresponding *mer* isomers (MIC = *ca.* 6.0 μg/ml). Overall, the excellent agreement of our findings with those reported for other families of Ru (II) polypyridyls[3] and, in particular for closely related Ru (II) pyridyl triazole complexes exposed to *S. aureus* and/or MRSA,[11a] suggests that also the "fully tetrazole" Ru (II) complexes described herein do most likely exert their antibacterial activity against *D. radiodurans* by targeting the bacterial cytoplasmic membrane. On these same premises, and beyond to supporting the possibility of getting useful insights for the determination of the structure to activity relationships that promote and govern the antibacterial properties of tris homoleptic Ru (II) complexes, our findings suggest how *Deinococcus radiodurans* might actually be considered as viable and non-pathogenic model Gram-positive bacteria in studies dealing with the search of new antimicrobials.

CCDC 1984712 contains the supplementary crystallographic data for *mer*-**[Ru (QTZ-Me)$_3$][PF$_6$]$_2$·CH$_3$CN**. These data can be obtained free of charge via http://www.ccdc.cam.ac.uk/conts/retrieving.html, or from the Cambridge Crystallographic Data Centre, 12 Union Road, Cambridge CB2 1EZ, UK; fax: (+44) 1223–336-033; or e-mail: deposit@ccdc.cam.ac.uk.

## 3.2 | Experimental section

### 3.2.1 | General considerations

All the reagents and solvents were obtained commercially (Sigma Aldrich/Merck, Alfa Aesar, Strem Chemicals) and used as received without any further purification, unless otherwise specified. All the reactions were carried out under an argon atmosphere following Schlenk protocols. The purification of the Ru (II) complexes was performed via column chromatography with the use of $SiO_2$ or $Al_2O_3$ as stationary phase. ESI-mass spectra were recorded using a Waters ZQ-4000 instrument (ESI-MS, acetonitrile as the solvent). Nuclear magnetic resonance spectra (consisting of $^1$H and $^{13}$C) were always recorded using a Varian Mercury Plus 400 ($^1$H, 399.9; $^{13}$C, 101.0 MHz). $^1$H and $^{13}$C chemical shifts were referenced to residual solvent resonances. Absorption spectra were recorded at 298 K using a Agilent Cary 100 UV–vis spectrometer.

## 3.3 | Cyclic voltammetry

$TBAPF_6$ (tetrabutylammonium hexafluorophosphate, Sigma Aldrich) was used as received as the supporting electrolyte, $CH_3CN$ was distilled over $CaH_2$ and thoroughly degassed under $N_2$ before each measurement. Electrochemical experiments were recorded with a Metrohm Autolab PGSTAT302N potentiostat-galvanostat using a Calomel electrode as reference (303/SCG/6 – Amel Electrochemistry) and a Platinum solid electrode (492/Pt/2 – Amel Electrochemistry) as working electrode.

## 3.4 | Ligand synthesis

Tetrazole derivatives are used as components for explosive mixtures.[10] In this lab, the reactions described here were only run on a few grams scale and no problems were encountered. However, *great caution* should be exercised when handling or heating compounds of this type.

Following the general method reported by Koguro and co-workers,[8] tetrazole ligand [H-**PTZ**] and [H-**QTZ**] were obtained in quantitative yield. [H-**PTZ**] $^1$H-NMR (DMSO $d^6$, 400 MHz) δ (ppm) = 8.82 (m, 1H); 8.25 (m, 1H); 8.10 (m, 1H); 7.66 (m, 1H); [H-**QTZ**] **$^1$H-NMR**, (DMSO-$d^6$, 400 MHz) δ (ppm) = 8,65 (d, 1H, $J_{H-H}$ = 8.79 Hz), 8,31 (d, 1H, $J_{H-H}$ = 8.40 Hz), 8,17 (d, 1H, $J_{H-H}$ = 8.40 Hz), 8,12 (d, 1H, $J_{H-H}$ = 7.99 Hz), 7,90 (t, 1H), 7.74 (t, 1H);

## 3.5 | Ligand functionalization

### 3.5.1 | General procedure for the preparation of [PTZ-me] and [QTZ-me][9a]

In a 100 ml two neck round bottomed flask equipped with a stirring bar were added 1 eq of the desired tetrazole ligand (H-QTZ, H-PTZ), 2 eq. of $CH_3I$ and 3 eq. of $K_2CO_3$ in 20 ml of $CH_3CN$. The mixture was heated at reflux for 24 hr. The mixture was then allowed to cool down to room temperature (hereafter, r.t.) and the solvent removed by rotary evaporation. The crude was dissolved in 10 mL of $CH_2Cl_2$ and filtered over a glass firt filter to remove the insoluble fraction. The soluble fraction was then purified with column chromatography over $SiO_2$ (PTZ-Me: Toluene/Acetone 9:1; QTZ-Me: hexane/EtOAc 6:4) yielding the desired N2 methylated isomer as second fraction (PTZ-Me: Y = 20%, 0.69 mmol; QTZ-Me: Y = 39%, 0.79 mmol).

**[PTZ-Me]**: **$^1$H-NMR**, 400 MHz, $CDCl_3$ δ (ppm): 8.77 (ddd, $J_{H-H}$ = 4.9, 1.8, 1.0 Hz, 1H), 8.23 (dt, $J_{H-H}$ = 7.9, 1.1 Hz, 1H), 7.86 (td, $J_{H-H}$ = 7.8, 1.8 Hz, 1H), 7.40 (ddd, $J_{H-H}$ = 7.6, 4.8, 1.2 Hz, 1H), 4.44 (s, 3H) **$^{13}$C-NMR**, 100 MHz, $CDCl_3$ δ (ppm): 164.93 ($C_t$), 150.21, 146.82, 137.22, 124.87, 122.35, 39.68.

**[QTZ-Me]**: **$^1$H-NMR**, 400 MHz, $CDCl_3$ δ (ppm): 8.25–8.21 (m, 1H), 7.74 (d,1 H, $J_{H-H}$ = 8.15 Hz), 7.70–7.66 (m, 1H), 7.50–7.46(m, 1H), 4.39 (s, 3H). **$^{13}$C-NMR**, 100 MHz, $CDCl_3$ δ (ppm): 164. 98 ($C_t$), 148.01, 146.49, 137.25, 130.01, 129.93, 128.32, 127.54, 127.42, 119.54, 39.71 ($CH_3$).

### 3.5.2 | General procedure for the preparation of [PTZ-$^t$Bu] and [QTZ-$^t$Bu][9b]

In a 50 ml two neck round bottomed flask equipped with a stirring bar was added the desired tetrazole ligand (H-QTZ, H-PTZ, 1 eq.) to 15 ml of tert-butanol in the presence of 3.0 ml of trifluoroacetic acid and 3.0 ml of concentrated sulphuric acid. The mixture was left to stir at r.t. overnight, during which time the initial suspension turned to a yellowish solution. Then, the mixture was poured into ice–water and made alkaline (pH > 12) by

the addition of KOH pellets. The resulting mixture was extracted with $CHCl_3$ (3 × 15 ml) and the organic layers were dried over $MgSO_4$. The solvent was then removed by rotary evaporation, providing the desired compound as an oily yellow residue (PTZ-$^t$Bu: Y = 77%, 2.53 mmol; QTZ-$^t$Bu: Y = 83% 1.27 mmol).

**[PTZ-$^t$Bu]**: **$^1$H-NMR**, 400 MHz, $CDCl_3$ δ (ppm): 8.80 (d, 1H, $J_{H-H}$ = 4.18 Hz), 8.27 (d, 1H, $J_{H-H}$ = 7.83 Hz), 7.86 (m, 1H), 7.39 (m, 1H), 1.83 (s, 9H).

**[QTZ-$^t$Bu]**: **$^1$H-NMR**, 400 MHz, $CDCl_3$ δ (ppm): 8.39–8.29 (m, 3H), 7.87 (ddd, $J_{H-H}$ = 8.3, 1.6, 0.7 Hz, 1H), 7.77 (ddd, $J_{H-H}$ = 8.5, 6.9, 1.5 Hz, 1H), 7.60 (ddd, $J_{H-H}$ = 8.1, 6.9, 1.2 Hz, 1H), 1.87 (s, 9H).

### 3.5.3 | General procedure for the preparation of [PTZ-hex] and [QTZ-hex][9c]

In 100 ml two neck round bottomed flask equipped with a stirring bar was added the desired tetrazole ligand (H-QTZ, H-PTZ, 1 eq.) to 30 ml of $CH_3CN$ in the presence of 1-bromohexane (1.1 eq) and $Et_3N$ (1.5 eq). The mixture was heated at reflux for 8 hr and then allowed to cool down to r.t. The crude product was then purified with column chromatography over $SiO_2$ (PTZ-Hex: Hexane/EtOAc 6:4; QTZ-Hex: Petroleum ether/EtOAc 9:1) yielding the desired N2-hexyl isomer as second fraction (PTZ-Hex: Y = 27%, 0.92 mmol; QTZ-Hex: Y = 14%, 0.69 mmol).

**[PTZ-Hex]**: **$^1$H-NMR**, 400 MHz, $CDCl_3$ δ (ppm): 8.71–8.69 (m, 1H), 8.18–8.15 (m, 1H), 7.98–7.75 (m, 1H), 7.32–7.28 (m, 1H), 4.64–4.60 (m, 2H), 2.03–1.95 (m, 2H), 1.30–1.16 (m, 6H), 0.80–0.76 (m, 3H). **$^{13}$C-NMR**, 100 MHz, $CDCl_3$ δ (ppm): 164.60 (Ct), 150.20, 146.84, 137.04, 124.69, 122.28, 53.45, 30.93, 29.22, 25.92, 22.27, 13.81.

**[QTZ-Hex]**: **$^1$H-NMR**, 400 MHz, $CDCl_3$ δ (ppm): 8.38–8.27 (m, 3H), 7.85 (dd, $J_{H-H}$ = 8.2, 1.4 Hz, 1H), 7.75 (ddd, $J_{H-H}$ = 8.5, 6.9, 1.5 Hz, 1H), 7.58 (ddd, $J_{H-H}$ = 8.1, 6.9, 1.1 Hz, 1H), 4.73 (t, $J_{H-H}$ = 7.3 Hz, 2H), 2.11 (p, $J_{H-H}$ = 7.4 Hz, 2H), 1.42–1.26 (m, 6H), 0.95–0.75 (m, 3H). **$^{13}$C-NMR**, 100 MHz, $CDCl_3$ δ (ppm): 164.83 (Ct), 148.09, 146.84, 137.38, 130.15, 128.44, 127.61, 127.51, 119.75, 53.61, 31.02, 29.38, 26.03, 22.36, 13.89.

## 3.6 | General procedure for the synthesis of homoleptic *fac-mer* $[Ru(N\,\widehat{N})_3]^{2+}$-type complexes

To a 7:3 solution of EtOH/$H_2O$ (30 ml) were added $RuCl_3$*x$H_2O$ (100 mg, 1 eq) and 3.2 eq of the desired 5-Aryltetrazole. The solution was stirred at reflux temperature overnight. The solvent was removed by rotary-evaporation and water was added (10 ml). Anion exchange was carried out by adding an excess of $NH_4PF_6$ (5 eq) to the solution and stirring for 1 hr. The solid product was isolated via vacuum filtration then washed with $H_2O$ and $Et_2O$.

***fac/mer*** **[Ru (PTZ-Me)$_3$]$^{2+}$** Y = 39% (MW = 874.16 g/mol, 0.0680 g, 0.0778 mmol, Column chromatography over $Al_2O_3$ eluted with DCM/ACN 1:1).

*fac:* **$^1$H-NMR**, 400 MHz, $CD_3CN$ δ (ppm): 8.48–8.43 (m, 3H), 8.26–8.19 (m, 3H), 7.98–7.95 (m, 3H), 7.65–7.60 (m, 3H), 4.42 (s, 9H) **$^{13}$C-NMR**, 100 MHz, $CD_3CN$ δ (ppm): 166.36 ($C_t$), 154.90, 147.40, 140.52, 129.84, 125.28, 42.97 ($CH_3$). **ESI-MS** (*m/z*): $[M]^{2+}$ = 292; $[M]^{2-}$ = 145 ($PF_6^-$). Anal. Calcd. For $C_{21}H_{21}N_{15}Ru_1P_2F_{12}$ (847.16) C 28.84, H 2.42, N 24.03. Found: C 27.54, H 2.42, N 21.90.

*mer:* **$^1$H-NMR**, 400 MHz, $CD_3CN$ δ (ppm): 8.46 (ddd, $J_{H-H}$ = 7.9, 1.5, 0.8 Hz, 1H), 8.39 (ddd, $J_{H-H}$ = 7.9, 1.5, 0.8 Hz, 1H), 8.36 (ddd, $J_{H-H}$ = 7.9, 1.5, 0.8 Hz, 1H), 8.23–8.08 (m, 4H), 8.00 (ddd, $J_{H-H}$ = 5.6, 1.4, 0.8 Hz, 1H), 7.80 (ddd, $J_{H-H}$ = 5.6, 1.4, 0.8 Hz, 1H), 7.60 (ddd, $J_{H-H}$ = 7.8, 5.7, 1.5 Hz, 1H), 7.52 (tdd, $J_{H-H}$ = 7.8, 5.6, 1.5 Hz, 2H), 4.46 (s, 3H), 4.45 (s, 3H), 4.41 (s, 3H). **$^{13}$C-NMR**, 100 MHz, $CD_3CN$ δ (ppm): 166.55 ($C_t$), 166.46 ($C_t$), 166.38 ($C_t$), 155.37, 155.26, 147.58, 147.56, 147.35, 140.40, 140.37, 140.30, 129.69, 129.1), 128.96, 125.56 (s), 124.94, 124.74, 42.99 ($CH_3$), 42.92 ($CH_3$), 42.91 ($CH_3$). **ESI-MS** (*m/z*): $[M]^{2+}$ = 292; $[M]^{2-}$ = 145 ($PF_6^-$). Anal. Calcd. For $C_{21}H_{21}N_{15}Ru_1P_2F_{12}$ (847.16) C 28.84, H 2.42, N 24.03. Found: C 28.16, H 2.42, N 22.91.

***fac/mer*** **[Ru (PTZ-$^t$Bu)$_3$]$^{2+}$** Y = 26% (MW = 1000.31 g/mol, 0.0937 g, 0.0937 mmol, Column chromatography over $Al_2O_3$ eluted with DCM/ACN 1:1).

*fac:* **$^1$H-NMR**, 400 MHz, $CD_3CN$ δ (ppm): 8.43–8.37 (m, 3H), 8.25–8.18 (m, 3H), 8.03–7.97 (m, 3H), 7.72–7.52 (m, 3H), 1.71 (s, 27H, $^t$Bu). **$^{13}$C-NMR**, 100 MHz, $(CD_3)_2O$ δ (ppm): 166.45 ($C_t$), 155.11, 148.06, 140.68, 130.10, 125.43, 69.50, 29.26 ($CH_3$). **ESI-MS** (*m/z*): $[M]^{2+}$ = 355; $[M]^{2-}$ = 145 ($PF_6^-$). Anal. Calcd. For $C_{30}H_{39}N_{15}Ru_1P_2F_{12}$ (1000.31) C 36.01, H 3.93, N 20.99. Found: C 36.89, H 4.06, N 21.51.

*mer:* **$^1$H-NMR**, 400 MHz, $CD_3CN$ δ (ppm): 8.44–8.34 (m, 2H), 8.34–8.29 (m, 1H), 8.22–8.08 (m, 3H), 7.96–7.93 (m, 1H), 7.88 (dt, $J_{H-H}$ = 5.4, 1.1 Hz, 1H), 7.85 (dt, $J_{H-H}$ = 5.5, 1.2 Hz, 1H), 7.61 (ddd, $J_{H-H}$ = 7.8, 5.6, 1.5 Hz, 1H), 7.56–7.46 (m, 2H), 1.75 (s, 9H), 1.73 (s, 9H), 1.71 (s, 9H). **$^{13}$C-NMR**, 100 MHz, $CD_3CN$ δ (ppm): 166.33 ($C_t$), 166.23 ($C_t$), 166.06 ($C_t$), 155.29, 155.12, 155.00, 148.02, 147.93, 147.81, 140.33, 140.21, 140.18, 129.74, 128.89, 125.34, 124.77, 124.57, 29.22 ($^t$Bu), 29.18 ($^t$Bu), 29.15 ($^t$Bu). **ESI-MS** (*m/z*): $[M]^{2+}$ = 355; $[M]^{2-}$ = 145 ($PF_6^-$). Anal. Calcd. For $C_{30}H_{39}N_{15}Ru_1P_2F_{12}$ (1000.31) C 36.01, H 3.93, N 20.99. Found: C 34.3, H 3.81, N 19.35.

***fac/mer* [Ru (PTZ-Hex)$_3$]$^{2+}$** Y = 52% (MW = 1,084 g/mol, 0.216 g, 0.199 mmol, Column chromatography over $Al_2O_3$ eluted with EtOAc/Acetone 8:2).

*fac:* **$^1$H-NMR**, 400 MHz, $CD_3CN$ δ (ppm): 8.75–8.73 (m, 3H), 8.19–8.16 (m, 3H), 7.96–7.94 (m, 3H), 7.51–7.43 (m, 3H), 4.75–4.69 (m, 6H), 2.06–1.98 (m, 6H) 1.36–1.27 (m, 18H), 0.90–0.87 (m, 9H). **$^{13}$C-NMR**, 100 MHz, $CD_3CN$ δ (ppm): 165.43 (Ct), 154.07, 146.57, 139.59, 128.91, 124.35, 55.90, 30.45, 28.36, 25.24, 22.06, 13.19. **ESI-MS** (*m/z*): $[M]^{2+}$ = 397; $[M]^{2-}$ = 145 ($PF_6^-$). Anal. Calcd. For $C_{36}H_{51}N_{15}Ru_1P_2F_{12}$ (1084.07) C 39.86, H 4.74, N 19.37. Found: C 40.98, H 5.03, N 18.38.

*mer:* **$^1$H-NMR**, 400 MHz, $CD_3CN$ δ (ppm): 8.47–8.44 (m, 1H), 8.41–8.39 (m, 1H), 8.38–8-34 (m, 1H), 8.23–8.13 (m, 3H), 8.05–8.04 (m, 1H), 7.95–7.94 (m, 1H), 7.85–7.84 (m, 1H), 7.63–7.59 (m, 1H), 7.55–7.51 (m, 2H), 4.77–4.71 (m, 6H), 2.03–1.99 (m, 6H), 1.35–1.25 (m, 18H), 0.90–0.84 (m, 9H). **$^{13}$C-NMR**, 100 MHz, $CD_3CN$ δ (ppm): 165.92 (Ct), 165.86 (Ct), 165.71 (Ct), 154.68, 154.53, 154.38, 147.07, 147.01, 146.88, 139.78, 139.73, 139.68, 129.07, 128.53, 128.30, 124.94, 124.35, 124.13, 56.35, 56.30, 56.09, 30.91, 30.82, 30.76, 28.75, 28.68, 28.52, 25.78, 25.71, 25.53, 22.37, 22.35, 22.31, 13.52, 13.50, 13.47. **ESI-MS** (*m/z*): $[M]^{2+}$ = 397; $[M]^{2-}$ = 145 ($PF_6^-$). Anal. Calcd. For $C_{36}H_{51}N_{15}Ru_1P_2F_{12}$ (1084.07) C 39.86, H 4.74, N 19.37. Found: C 40.43, H 4.89, N 18.86.

***fac/mer* [Ru (QTZ-Me)$_3$]$^{2+}$** Y = 49% (MW = 1024.21 g/mol, 0.0923 g, 0.0895 mmol, Column chromatography over $Al_2O_3$ eluted with DCM/ACN 1:1). *fac:* **$^1$H-NMR**, 400 MHz, $(CD_3)_2CO$ δ (ppm): 9.07 (dd, $J_{H-H}$ = 8.6, 0.8 Hz, 3H), 8.69 (d, $J_{H-H}$ = 8.4 Hz, 3H), 8.34 (dd, $J_{H-H}$ = 8.2, 1.5 Hz, 3H), 8.10 (dd, $J_{H-H}$ = 8.9, 0.9 Hz, 3H), 7.76 (ddd, $J_{H-H}$ = 8.1, 6.9, 1.0 Hz, 3H), 7.26 (ddd, $J_{H-H}$ = 8.7, 7.0, 1.5 Hz, 3H), 4.52 (s, 9H, $CH_3$). **$^{13}$C-NMR**, 100 MHz, (CD3)$_2$O δ (ppm):168.01 ($C_t$), 150.94, 148.90, 143.24, 134.01, 131.46, 131.42, 130.76, 130.76, 127.26, 120.82, 43.14 ($CH_3$). **ESI-MS** (*m/z*): $[M]^{2+}$ = 367; $[M]^{2-}$ = 145 ($PF_6^-$). Anal. Calcd. For $C_{33}H_{27}N_{15}Ru_1P_2F_{12}$ (1024.21) C 38.68, H 2.66, N 20.50. Found: C 39.45, H 2.84, N 21.03.

*mer:* **$^1$H-NMR**, 400 MHz, $CD_3CN$ δ (ppm): 8.77 (dd, $J_{H-H}$ = 8.5, 0.9 Hz, 1H), 8.67–8.59 (m, 2H), 8.45 (d, $J_{H-H}$ = 8.5 Hz, 1H), 8.33 (d, $J_{H-H}$ = 8.4 Hz, 1H), 8.27 (d, $J_{H-H}$ = 8.4 Hz, 1H), 8.15–8.09 (m, 2H), 8.03 (dd, $J_{H-H}$ = 8.2, 1.5 Hz, 1H), 7.77 (ddd, $J_{H-H}$ = 8.1, 7.0, 1.1 Hz, 1H), 7.71–7.55 (m, 3H), 7.56–7.42 (m, 2H), 7.17 (dd, *J* = 8.9, 0.9 Hz, 1H), 7.05 (ddd, *J* = 8.8, 6.9, 1.5 Hz, 1H), 6.68 (dd, $J_{H-H}$ = 8.9, 0.9 Hz, 1H), 4.49 (s, 3H), 4.44 (s, 3H), 4.40 (s, 3H). **$^{13}$C-NMR**, 100 MHz, $(CD_3)_2O$ δ (ppm): 167.65, 167.16, 166.58, 150.55, 150.44, 149.82, 149.05, 148.80, 148.10, 133.86, 133.32, 132.62, 130.51, 130.19, 130.04, 129.83, 129.74, 129.62, 129.55, 125.59124.68, 124.11, 119.59, 119.45, 119.16, 42.33, 42.30, 42.27. **ESI-MS** (*m/z*): $[M]^{2+}$ = 367; $[M]^{2-}$ = 145 ($PF_6^-$). Anal. Calcd. For $C_{33}H_{27}N_{15}Ru_1P_2F_{12}$ (1024.21) C 38.68, H 2.66, N 20.50. Found: C 39.45, H 2.84, N 21.03.

***fac/mer* [Ru (QTZ-$^t$Bu)$_3$]$^{2+}$** Y = 47% (MW = 1,150 g/mol, 0.207 g, 0.180 mmol, Column chromatography over $SiO_2$ eluted with $CH_3CN/H_2O/KNO_{3(aq)}$ 20:1:0.1. Counterion exchange was carried out by stirring overnight ***fac*** and ***mer* [Ru (QTZ-Hex)$_3$]$^{2+}$** in a saturated $CH_2Cl_2/KPF_6$ solution).

*fac:* **$^1$H-NMR**, 400 MHz, $CD_3CN$ δ (ppm): 9.81–9.79 (d, $J_{H-H}$ = 7.9 Hz, 3H), 8.52–8.50 (d, $J_{H-H}$ = 7.9 Hz, 3H), 8.30–8.28 (d, $J_{H-H}$ = 7.9 Hz, 3H), 8.14–8.10 (m, 3H), 8.04–7.99 (m, 3H), 7.89–7.85 (m, 3H), 1.80 (s, 27H). **$^{13}$C-NMR**, 100 MHz, $CD_3CN$ δ (ppm): 168.43 (Ct), 151.48, 149.95, 140.18, 130.33, 129.43, 128.30, 128.12, 127.04, 118.52, 68.02, 28.07. **ESI-MS** (*m/z*): $[M]^{2+}$ = 430; $[M]^{2-}$ = 145 ($PF_6^-$). Anal. Calcd. For $C_{42}H_{45}N_{15}Ru_1P_2F_{12}$ (1150) C 43.83, H 3.94, N 18.25. Found: C 43.16, H 4.05, N 17.97.

*mer:* **$^1$H-NMR**, 400 MHz, $CD_3CN$ δ (ppm): 8.78–8.76 (d, $J_{H-H}$ = 7.9 Hz, 1H), 8.56–8.62 (m, 2H), 8.45–8.43 (d, $J_{H-H}$ = 7.9 Hz, 1H), 8.32–8.30 (d, $J_{H-H}$ = 7.9 Hz, 1H), 8.22–8.20 (d, $J_{H-H}$ = 7.9 Hz, 1H), 8.18–8.15 (m, 1H), 8.12–8.06 (m, 2H), 8.05–7.77 (m, 1H), 7.70–7.53 (m, 4H), 7.46–7.42 (m, 1H), 7.06–7.02 (m, 1H), 6.97–6.95 (m, 1H), 6.69–6.67 (m, 1H), 1.77 (s, 9H), 1.72 (s, 9H), 1.67 (s, 9H). **$^{13}$C-NMR**, 100 MHz, $CD_3CN$ δ (ppm): 166.94, 166.61, 166.20, 150.65, 150.63, 150.26, 149.85, 149.60, 149.13, 148.51, 148.04, 141.80, 141.72, 141.49, 133.17, 132.81, 132.62, 132.33, 130.28, 130.06, 129.87, 129.75, 129.70, 128.02, 126.66, 125.99, 124.36, 119.87, 119.52119.46, 69.32, 69.27, 68. 88, 28.36, 28.24, 28.19. **ESI-MS** (*m/z*): $[M]^{2+}$ = 430; $[M]^{2-}$ = 145 ($PF_6^-$). Anal. Calcd. For $C_{42}H_{45}N_{15}Ru_1P_2F_{12}$ (1150) C 43.83, H 3.94, N 18.25. Found: C 44.34, H 4.06, N 18.8.

***fac/mer* [Ru (QTZ-Hex)$_3$]$^{2+}$** Y = 59% (MW = 1,234 g/mol, 0.279 g, 0.226 mmol, Column chromatography over $SiO_2$ eluted with $CH_3CN/H_2O/KNO_{3(aq)}$ 20:1:0.1. Counterion exchange was carried out by stirring overnight ***mer* [Ru (QTZ-Hex)$_3$]$^{2+}$** in a saturated $CH_2Cl_2/KPF_6$ solution).

*fac:* **$^1$H-NMR**, 400 MHz, $CD_3CN$ δ (ppm): not isolated.

*mer:* **$^1$H-NMR**, 400 MHz, $CD_3CN$ δ (ppm): 8.76–8.70 (m, 3H), 8.46–8.44 (m, 1H), 8.41–8.39 (m, 1H), 8.31–8.29 (m, 1H), 8.21–8.19 (m, 1H), 8.11–8.08 (m, 1H), 7.83–7.80 (m, 1H), 7.70–7.60 (m, 3H), 7.46–7.39 (m, 1H), 7.15–7.13 (m, 1H), 7.04–7.00 (m, 1H), 6.70–6.68 (m, 1H), 4.77–4.68 (m, 6H), 2.15–1.90 (m, 10H), 1.31–1.11 (m, 16H), 0.88–0.78 (m, 9H). **$^{13}$C-NMR**, 100 MHz, $CD_3CN$ δ (ppm): 167.56, 167.07, 166.41, 150.85, 150.30, 150.17, 149.29, 148.84, 148.35, 141.90, 141.73, 141.65, 133.71, 133.09, 132.48, 130.61, 130.28, 130.19, 129.94, 129.88, 129.83,

129.61, 129.52, 125.39, 124.60, 124.35, 119.81, 119.43, 119.33, 117.29, 56.47, 56.22, 56.07, 30.46, 30.44, 30.30, 28.46, 28.39, 28.32, 25.40, 25.31, 25.05, 22.06, 22.03, 22.1, 13.19, 13.17. 13.15. **ESI-MS** (*m/z*): $[M]^{2+}$ = 472; $[M]^{2-}$ = 145 ($PF_6^-$). Anal. Calcd. For $C_{48}H_{57}N_{15}Ru_1P_2F_{12}$ (1234) C 46.68, H 4.65, N 17.01. Found: C 47.06, H 4.74, N 17.56.

## 3.7 | Disk diffusion test

The antimicrobial activity of *fac/mer* $[Ru(N\,\hat{N})_3]^{2+}$ complexes was evaluated by using the disk diffusion test in agar plates. Single colonies of *Escherichia coli* TOP10 and *Deinococcus radiodurans* DSM 46620 were grown in LB (10 g/l tryptone, 5 g/L yeast extract, 10 g/l NaCl) and TGY (5 g/l tryptone, 3 g/l yeast extract, 1 g/l glucose) liquid medium at 37 or 30 °C, respectively. After overnight incubation, 0.1 ml of each bacterial suspension (approximately $1x10^7$ CFU) was spread onto LB-agar and YPD-agar plates (1.5% agar), respectively. Sterile paper disks (diameter: 1 cm, 4 disks per plate) impregnated individually with 20 μL of each ruthenium (II) compound (1 mg/1 ml DMSO) were placed on each plate. All plates included an ampicillin-disk as positive control (100 μg/ml) and a DMSO alone-disk (20 μL) as negative control. After incubation for 24 hr at the proper temperature (30 °C for *D. radiodurans* and 37 °C for *E. coli*), the presence of inhibition zones of bacterial growth was evaluated.

## 3.8 | Bacterial growth curves

Single colonies of *E. coli* were grown in LB medium (2 ml) at 37 °C under shaking for 15 hr. The inoculum of *D. radiodurans* was prepared by growing a single colony in 5 ml of TGY broth at 30 °C for 24 hr under shaking. Each pre-culture was diluted to 0.05 optical density at 600 nm ($OD_{600nm}$) into fresh LB and TGY medium (5 ml), respectively, and the kinetics of growth was measured at appropriate time intervals by reading the optical density at 600 nm using a plastic cuvette in a spectrophotometer (GeneQuant, Amersham Pharmacia). 5 μM and 20 μM of *fac/mer* $[Ru(N\,\hat{N})_3]^{2+}$ complexes were separately added to *E. coli* or *D. radiodurans* cultures. Control cultures treated with DMSO alone (2%) were performed.

## 3.9 | Determination of MIC

The minimal inhibitory concentration (MIC) was determined by the broth dilution method using different concentrations of *fac/mer*-**[Ru (PTZ-R)$_3$]$^{2+}$** and *fac/mer*-**[Ru (QTZ-R)$_3$]$^{2+}$** complexes. In detail, independent cultures of *D. radiodurans* (5 mL TGY), prepared as described before, were incubated with proper dilutions of *fac/mer*-**[Ru (PTZ-R)$_3$]$^{2+}$** and *fac/mer*-**[Ru (QTZ-R)$_3$]$^{2+}$**complexes in order to obtain final concentrations ranging from 0 to 5 μM. The dilutions of ruthenium (II) complexes were performed in DMSO. The MIC was determined as the lowest concentration of *fac/mer*-**[Ru (PTZ-R)$_3$]$^{2+}$** and *fac/mer*-**[Ru (QTZ-R)$_3$]$^{2+}$** complexes able to inhibit microbial growth. The rate of bacterial growth was evaluated by measuring the turbidity as described before. A control culture containing DMSO alone was also prepared.

## 3.10 | X-ray crystallography

Crystal data and collection details for *mer*-**[Ru (QTZ-Me)$_3$][PF$_6$]$_2$·CH$_3$CN** are reported in Table 1 and S2 ESI. The diffraction experiments were carried out on a Bruker APEX II diffractometer equipped with a PHOTON100 detector and using Mo-Kα radiation. Data were corrected for Lorentz polarization and absorption effects (empirical absorption correction SADABS).[17] Structures were solved by direct methods and refined by full-matrix least-squares based on all data using $F^2$.[18] H-atoms were placed in calculated positions, and refined isotropically using a riding model. All non-hydrogen atoms were refined with anisotropic displacement parameters.

**Supporting Information (SI †)** available: ESI-MS and NMR ($^1$H, $^{13}$C,) spectra of all the complexes. Absorption spectra and relative data, CV data. Crystallographic data for *mer*-**[Ru (QTZ-Me)$_3$][PF$_6$]$_2$·CH$_3$CN**.

## ACKNOWLEDGEMENTS

The authors wish to thank the Italian Ministry of Education, University and Research (MIUR) for financial support (PRIN project: Towards a Sustainable Chemistry: Design of Innovative Metal–Ligand Systems for Catalysis and Energy Applications, PRIN 2015 20154X9ATP_003).

## CONFLICTS OF INTERESTS

There are no conflicts to declare.

## ORCID

*Nicola Monti* https://orcid.org/0000-0003-1272-931X
*Stefano Zacchini* https://orcid.org/0000-0003-0739-0518
*Massimiliano Massi* https://orcid.org/0000-0001-6949-4019
*Alejandro Hochkoeppler* https://orcid.org/0000-0002-5144-2154
*Loris Giorgini* https://orcid.org/0000-0003-2248-3552

*Valentina Fiorini* https://orcid.org/0000-0003-0467-6705
*Alessandra Stefan* https://orcid.org/0000-0003-0391-7474
*Stefano Stagni* https://orcid.org/0000-0002-7260-4845

## REFERENCES

[1] a) S. Campagna, F. Puntoriero, F. Nastasi, G. Bergamini, V. Balzani, *Top. Curr. Chem.* **2007**, *280*, 117. b) M. D. K. Nazeeruddin, E. Baranoff, M. Grätzel, *Solar Energy* **2011**, 85.

[2] a) J. Shum, P. K.-K. Leung, K. K.-W. Lo, *Inorg. Chem.* **2019**, *58*, 2231. and references cited therein b) Q. Zhao, C. Huang, F. Li, *Chem. Soc. Rev.* **2011**, *40*, 2508. and references cited herein

[3] F. Li, J. G. Collins, F. R. Keene, *Chem. Soc. Rev.* **2015**, *44*, 2529. and references cited herein

[4] a) F. Dwyer, E. C. Gyarfas, W. P. Rogers, J. H. Koch, *Nature* **1952**, *170*, 190. b) F. Dwyer, I. K. Reid, A. Shulman, G. M. Laycock, S. Dixson, *Immunol. Cell Biol.* **1969**, *47*, 203.

[5] F. Li, Y. Mulanya, M. Feterl, J. M. Warner, J. G. Collins, F. R. Keene, *Dalton Trans.* **2011**, *40*, 5032.

[6] a) L. Lu, L.–. J. Liu, W.-C. Chao, H.-J. Zhong, M. Wang, X.-P. Chen, J.-J. Lu, R.-N. Li, D.-L. Ma, C.-H. Leung, *Sci. Rep.* **2015**, *5*, 14544. see also:b) J. A. Lemire, J. J. Harrison, R. J. Turner, *Nat. Rev. Microbiol. 2013*, 371.

[7] a) S. V. Kumar, S. Ø. Scottwell, E. Waugh, C. J. McAdam, L. R. Hanton, H. J. L. Brooks, J. D. Crowley, *Inorg. Chem.* **2016**, *55*, 9767. b) Q. V. C. van Hilst, R. A. S. Vasdev, D. Preston, J. A. Findlay, S. Ø. Scottwell, G. I. Giles, H. J. L. Brooks, J. D. Crowley, *Asian J. Org. Chem.* **2019**, *8*, 496.

[8] a) N. Akabar, V. Chaturvedi, G. E. Shillito, B. J. Schwehr, K. C. Gordon, G. S. Huff, J. J. Sutton, B. W. Skelton, A. N. Sobolev, S. Stagni, D. J. Nelson, M. Massi, *Dalton Trans.* **2019**, *48*, 15613. b) M. J. Stout, A. Stefan, B. W. Skelton, A. N. Sobolev, M. Massi, A. Hochkoeppler, S. Stagni, P. V. Simpson, *Eur. J. Inorg. Chem.* **2020**, 292. c) A. Sorvina, C. A. Bader, J. R. T. Darby, M. C. Lock, J. Y. Soo, I. R. D. Johnson, C. Caporale, N. H. Voelcker, S. Stagni, M. Massi, J. L. Morrison, S. E. Plush, D. A. Brooks, *Sci. Rep.* **2018**, *8*, 8191. d) V. Fiorini, L. Bergamini, N. Monti, S. Zacchini, S. E. Plush, M. Massi, A. Hochkoeppler, A. Stefan, S. Stagni, *Dalton Trans.* **2018**, *47*, 9400. e) C. Caporale, C. A. Bader, A. Sorvina, K. D. M. MaGee, B. W. Skelton, T. A. Gillam, P. J. Wright, P. Raiteri, S. Stagni, J. L. Morrison, S. E. Plush, D. A. Brooks, M. Massi, *Chem. – Eur. J.* **2017**, *23*, 15666. and references cited therein

[9] A. M. Ranieri, C. Caporale, V. Fiorini, A. Hubbard, P. Rigby, S. Stagni, E. Watkin, M. I. Ogden, M. J. Hackett, M. Massi, *Chem. – Eur. J.* **2019**, *25*, 10566.

[10] V. Fiorini, I. Zanoni, S. Zacchini, A. L. Costa, A. Hochkoeppler, V. Zanotti, A. M. Ranieri, M. Massi, A. Stefan, S. Stagni, *Dalton. Trans.* **2017**, *46*, 12328.

[11] a) D. Slade, M. Radman, *Microbiol. Mol. Biol. Rev.* **2011**, *75*, 133. b) L. Wei, M. Yun, X. Fangzhu, H. Shuya, *Adv. Nat. Sci.* **2014**, *7*, 6.

[12] K. Koguro, T. Oga, S. Mitsui, R. Orita, *Synthesis* **1998**, 910.

[13] a) R. A. Henry, *J. Am. Chem. Soc.* **1951**, *73*, 4470. b) C. Femoni, S. Muzzioli, A. Palazzi, S. Stagni, S. Zacchini, F. Monti, G. Accorsi, M. Bolognesi, N. Armaroli, M. Massi, G. Valenti, M. Marcaccio, *Dalton. Trans.* **2013**, *42*, 997. c) U. Sheridan, J. McGinley, J. F. Gallagher, A. Fleming, F. Kelleher, *Polyhedron* **2013**, *59*, 8.

[14] R. N. Butler, Tetrazoles, in *Comprehensive Heterocyclic Chemistry II*, (Ed: R. C. Storr) Vol. 4, Pergamon Press, Oxford **1996** 621 and references cited therein.

[15] F. Puntoriero, F. Nastasi, M. Galletta, S. Campagna, *Photophysics and Photochemistry of Non-Carbonyl-Containing Coordination and Organometallic Compounds*, Vol. 8, Elsevier **2013** 255.

[16] As suggested by one Reviewer, further experiments aimed at evaluating the mimimum bactericidal concentration (MBC) of all complexes and, consequently, their bacteriostatic or bactericidal character, will be performed soon and will become as one of our standard procedures.

[17] G. M. Sheldrick, *SADABS-2008/1 – Bruker AXS Area Detector Scaling and Absorption Correction*, Bruker AXS, Madison, WI **2008**.

[18] G. M. Sheldrick, *Acta Crystallogr. C* **2015**, *71*, 3.

## SUPPORTING INFORMATION

Additional supporting information may be found online in the Supporting Information section at the end of this article.

**How to cite this article:** Monti N, Zacchini S, Massi M, et al. Antibacterial activity of a new class of tris homoleptic Ru (II)-complexes with alkyl-tetrazoles as diimine-type ligands. *Appl Organomet Chem*. 2020;e5806. https://doi.org/10.1002/aoc.5806